UC Irvine

Title

Lysosomal Dysfunction Results in Lamina-Specific Meganeurite Formation but Not Apoptosis in Frontal Cortex

Permalink

https://escholarship.org/uc/item/0j35j8d1

Journal

ISSN

Authors

Yong, Alex P
Bednarski, Eric
Gall, Christine M
et al.

Publication Date

1999-05-01

DOI

Copyright Information

Peer reviewed

Lysosomal Dysfunction Results in Lamina-Specific Meganeurite Formation but Not Apoptosis in Frontal Cortex

Alex P. Yong,* Eric Bednarski,† Christine M. Gall,* Gary Lynch,†,‡ and Charles E. Ribak*

*Department of Anatomy and Neurobiology, †Center for the Neurobiology of Learning and Memory,
and ‡Department of Psychiatry, University of California, Irvine, California 92697

An inhibitor of cathepsins B and L was used to test if lysosomal dysfunction in cultured slices of rat frontal cortex induces pathological features that develop in the human cortex during aging and Alzheimer's disease (AD). Incubation for 6 days with *N*-CBZ-ʟ-phenyl-alanyl-ʟ-alanine-diazomethylketone (ZPAD) resulted in a massive proliferation of endosomes-lysosomes in all cortical layers. Slices additionally exposed to a washout of 4 days had numerous meganeurites, blister-like structures in the region of the axon hillock, in layer III but not in other cortical laminae. Meganeurites are a characteristic feature of the human frontal cortex after age 50 and are largely restricted to layer III. Tests for apoptosis were carried out at two intervals following meganeurite formation. TUNEL-labeled neurons were confined to layers II/III on the surface of the slices but there was no evidence for a ZPAD effect. In all, 6 days of lysosomal dysfunction reproduces characteristic effects of normal aging in neocortex without generating some key features of AD. © 1999 **Academic Press**

Key Words: brain aging; Alzheimer's disease; lysosomes; cathepsins; meganeurites; apoptosis

INTRODUCTION

Large fusiform expansions interposed between the base of the perikaryon and the initial portion of the axon commonly occur in areas of the aged human brain (5). These "meganeurites" are present in frontal cortex by age 50, increase in number to at least age 70, are prominent in layer III pyramidal cells but not in neurons of other cortical lamina, and are filled with lipofuscin and other complex lysosomal organelles (5). The location and appearance of meganeurites suggest that lysosomes gradually accumulate during human aging within abnormal processes that can negatively affect the integrity of somatoaxonal communication. Accordingly, their origins, and the reasons meganeurites develop in only select collections of neurons, are questions of considerable interest.

Given the findings noted above, it is possible that the proliferation of lysosomes which accompanies aging (16, 22) contributes importantly to meganeurite formation. Evidence in favor of this was obtained using experimentally induced lysosomal dysfunction. Specifically, selective inhibitors of cathepsins B and L caused a massive proliferation of lysosomal organelles in long-term cultures of rat hippocampal slices (3). The increased number of lysosomes developed within 1 day and was followed by the appearance of cathepsin D in the extralysosomal (cytoplasmic) compartment (2). Between 1 and 2 weeks later, meganeurites of the type found in the human brain—but not reported for rats—were observed in the CA1 subfield (3). This event was correlated with a marked reduction in lysosomes in the somata of meganeurite containing pyramidal cells. Thus, it appeared that meganeurites were generated by accumulations of excess lysosomes transported to the basal pole of neurons.

The present studies further investigated the degree to which selective lysosomal disturbances induce specialized signs of human brain aging and asked if this extends to concommitants of Alzheimer's disease (AD). As noted, meganeurites in the superior frontal cortex are restricted to layer III (5), although lysosomal proliferation occurs across laminae. One set of experiments was intended to provide a first test of whether cathepsin inhibitors reproduce this human pattern in cultured slices of rat frontal cortex. Additional experiments examined the possibility that lysosomal dysfunction also causes apoptotic cell death in cortical slices. Several studies have shown that DNA breaks and fragmentation in the cerebral and entorhinal cortices are far more common in advanced AD than in age matched controls (1, 17, 21). The differences from controls are sufficiently great that cortical apoptosis has been proposed to be a possible mechanism of cell death in AD (10, 21). It was of interest therefore to determine if lysosomal dysfunction generates TUNEL-positive profiles in the same areas in which it triggers meganeurite formation.

150

MATERIALS AND METHODS

Cultured neocortical slices. Neocortical slices were prepared from 6- to 8-day-old Sprague–Dawley rats. Pups were killed by decapitation under light isoflurane anesthesia. The brains were removed from the cranium and immediately submerged in a solution of artificial CSF composed of 124 mM NaCl, 3 mM KCl, 1.25 mM KH_2PO_4, 4 mM $MgSO_4$, 2 mM $CaCl_2$, 25 mM $NaHCO_3$, 20 mM D-glucose, 5 mM Hepes buffer, 100 µM adenosine, and 0.5 mM ascorbate, pH 7.20. Subsequently, with brains placed on their dorsal surface, a razor blade was used to block the tissue in the coronal plane with cuts placed 1 and 6 mm posterior to the frontal pole. This tissue block was then placed on its anterior cut surface and one cut was made beneath the cortical white matter to remove the underlying striatal tissue. The remaining tissue was placed on its ventral cut surface and two additional cuts were made to isolate frontal cortex from cingulate and parietal cortices. Frontal cortical slices were then prepared from the resulting block by sectioning at a thickness of 400 µm in the coronal plane using a McIlwain tissue chopper. The cortical slices were transferred to the membranes of Millicell-CM culture inserts (Millipore Corp.) in six-well culture cluster plates with two to three slices per insert, six inserts per culture plate, and 1 ml media per well using methods described by Stoppini *et al.* (20). The upper surfaces of the slices were exposed to a humidified, 37°C atmosphere containing 5% CO_2. The culture medium was previously described (3). Slices were maintained *in vitro* at least 9 days before experiments were started with a media exchange every 2 days. Each culture plate contained explants from only one animal and individual wells were used for matched control and experimental treatment groups.

Experiments were initiated by exposing a subset of cultured slices of frontal cortex with 45 µM *N*-CBZ-L-phenylalanyl-L-alanine-diazomethylketone (ZPAD; BACHEM Bioscience, Inc., Torrance, CA), an inhibitor of cathepsins B and L (13) or vehicle (dimethyl sulfoxide; DMSO). The drug (or DMSO) was diluted in regular culture medium (as above except for the fact that the horse serum was heat inactivated at 56°C for 35 min prior to use) and applied with a full 1-ml media exchange. The treatment medium was replenished every 2 days.

The first set of cortical slices were exposed to the inhibitor ($n = 19$) or vehicle ($n = 17$) for a total of 6 days before being fixed and processed for electron microscopy. Additional sets of vehicle/control and ZPAD-treated slices were exposed to the vehicle or drug for 6 days and then transferred to fresh culture media (without ZPAD or DMSO) for either (1) an additional 4 days before fixation for electron microscopy (9 ZPAD-treated and 10 control slices), or (2) an additional 7 or 12 days before fixation for TUNEL staining (17 ZPAD-treated and 14 yoked control slices per interval).

Electron microscopy. Control and ZPAD-treated slices were fixed in an ice-cold solution of 0.1 M phosphate buffer (pH 7.4) (PB), 1.5% paraformaldehyde, and 1.5% glutaraldehyde. After 2 h, this solution was aspirated and slices were washed three times in phosphate-buffered saline (PBS; 50 mM phosphate buffer, 0.9% NaCl, pH 7.3). Slices were postfixed in 2% osmium tetroxide in PB for 1 h, dehydrated in a series of graded alcohols, and embedded in Polybed-812. Semithin (1 µm) sections were cut from these blocks and stained with 0.1% toluidine blue. These sections were used to identify the various layers of frontal cortex. Since these slices were obtained from agranular frontal cortex, only five layers (i.e., layers I, II, III, V, and VI) could be identified. Thin sections were taken from either superficial or deep layers to examine the ultrastructure of pyramidal neurons at different depths. After trimming the specimen, thin sections were cut with a diamond knife, mounted on Formvar-coated slot grids, stained with uranyl acetate and lead citrate, and examined with a Philips CM10 electron microscope.

Terminal deoxynucleotidyl transferase-mediated dUTP-biotin nick end labeling (TUNEL) assay. Control and ZPAD-treated slices were fixed in 4% paraformaldehyde in PB (overnight, 4°C), cryoprotected in 20% sucrose/4% paraformaldehyde (1 h, 4°C), sectioned on a freezing microtome (20 µm thick, parallel to the broad explant surface), and collected into 4% paraformaldehyde in cold PB. Sections were then mounted onto sterile Fisher Superfrost/Plus slides, air dried, and processed for TUNEL staining. Sections were rinsed in PB and glycine/0.1 M PB at room temperature (RT), for 5 min each, dehydrated through increasing ethanols, defatted in chloroform (10 min), and rehydrated through decreasing ethanols. The slices were then treated with 0.25% acetic anhydride (15 min, RT), rinsed in PBS, and incubated in terminal deoxynucleotidyl transferase buffer (30 mM Tris–HCl, 140 mM Na cacodylate, 1 mM $CoCl_2$, pH 7.2) containing 25 units/ml terminal deoxynucleotidyl transferase, 0.2 mg/ml bovine serum albumin, and 0.25 µM digoxigenin-labeled-UTP (DIG-11-dUTP) (2 h, 37°C). The tissue was then washed in descending concentrations of saline sodium citrate (SSC: 150 mM NaCl, 15 mM Na citrate, pH 7.0) buffer to a final wash in 0.1 × SSC at RT and incubated in 0.1 × SSC containing 2% normal sheep serum (NSS) (1 h, RT). Sections were then incubated with a sheep anti-DIG antiserum (Boehringer-Mannheim) diluted 1:2000 in Tris-buffered saline (TBS: 100 mM Tris–HCl, 150 mM NaCl, pH 7.5), containing 2% NSS, and 0.05% Triton-X 100 (overnight, RT). The following day, the tissue was washed in TBS and Tris–$MgCl_2$ (100 mM Tris–HCl, 100 mM NaCl, 50 mM $MgCl_2$, pH 9.5) and then incubated in Tris–$MgCl_2$ containing nitroblue

tetrazolium (0.34 mg/ml), 5 bromo-4-chloro-3-indolyl phosphate (0.18 mg/ml), and levamisole (0.24 mg/ml) in the dark for 2 h at RT. After this color reaction, the tissue was rinsed in 10 mM Tris–HCl/1 mM EDTA, pH 8.0, dehydrated through ascending alcohols and clearing solvent (Stephens Scientific) and coverslips were applied with Permount.

RESULTS

Morphology of cultured neocortical slices. Slices obtained from the frontal cortex and maintained *in vitro* for 15–21 days had laminar cytoarchitectural features similar to those found *in vivo* (8, 9, 11). Five distinct layers could be discriminated in toluidine blue-stained semithin sections (Fig. 1A). Layer I was cell poor and located below a pial surface coated with astrocytes and above sizable populations of small and medium-sized pyramidal shaped neurons. A gradient existed with small pyramidal neurons lying just beneath the easily defined layer I and medium-sized cells positioned deeper, corresponding to the arrangements of layers II and III *in vivo* (15). As shown in Fig. 1B, the deeper medium-sized neurons had apically oriented primary dendrites and perikarya resembling those of layer III pyramidal cells. A thin but clearly cell sparse, horizontal strip was present below the lower boundary of the field of medium-sized pyramidal cells in layer III and
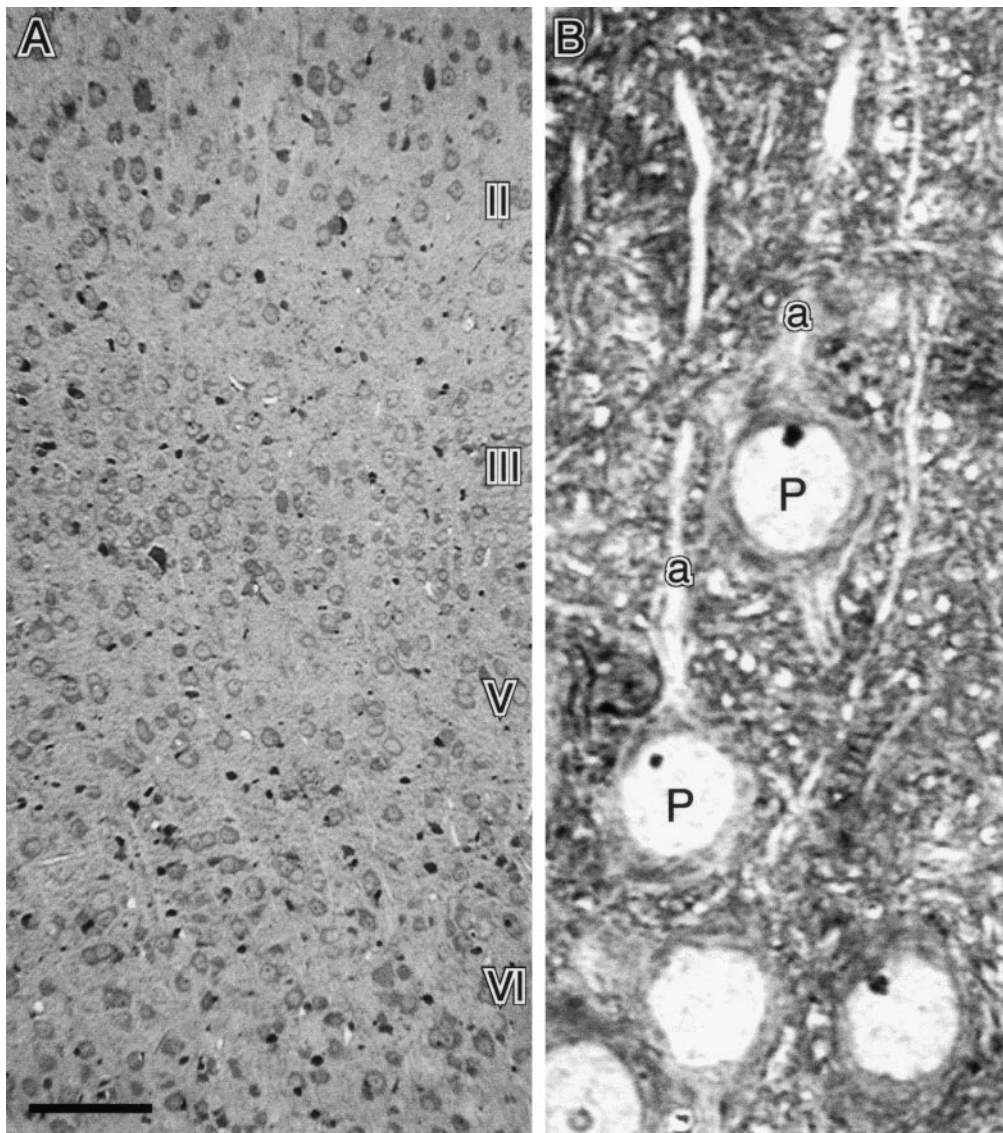

FIG. 1. Light micrographs of semithin sections stained with toluidine blue from a control cultured frontal cortical slice maintained *in vitro* for 17 days. (A) Layers II, III, V, and VI in the typical lamination pattern for this region. (B) An enlargement of a group of layer III neurons. Pyramidal cells (P) show round nuclei and apical dendrites (a) pointing toward the pial surface. There are very few basophilic organelles located in these neurons. Bar, 75 μm in A and 10 μm in B.

above the superficial border of a diffuse layer of larger neurons. The size, appearance, and packing densities of the latter neurons were typical for layer V pyramidal neurons in the rat. Nonpyramidal cells were also present but were not examined in any detail.

The ultrastructure of cortical neurons in control slices was unremarkable. Cellular organelles including Golgi complexes, granular endoplasmic reticulum, Nissl bodies, mitochondria, and polyribosomes (Fig. 2) were comparable to their counterparts in the cortex of young
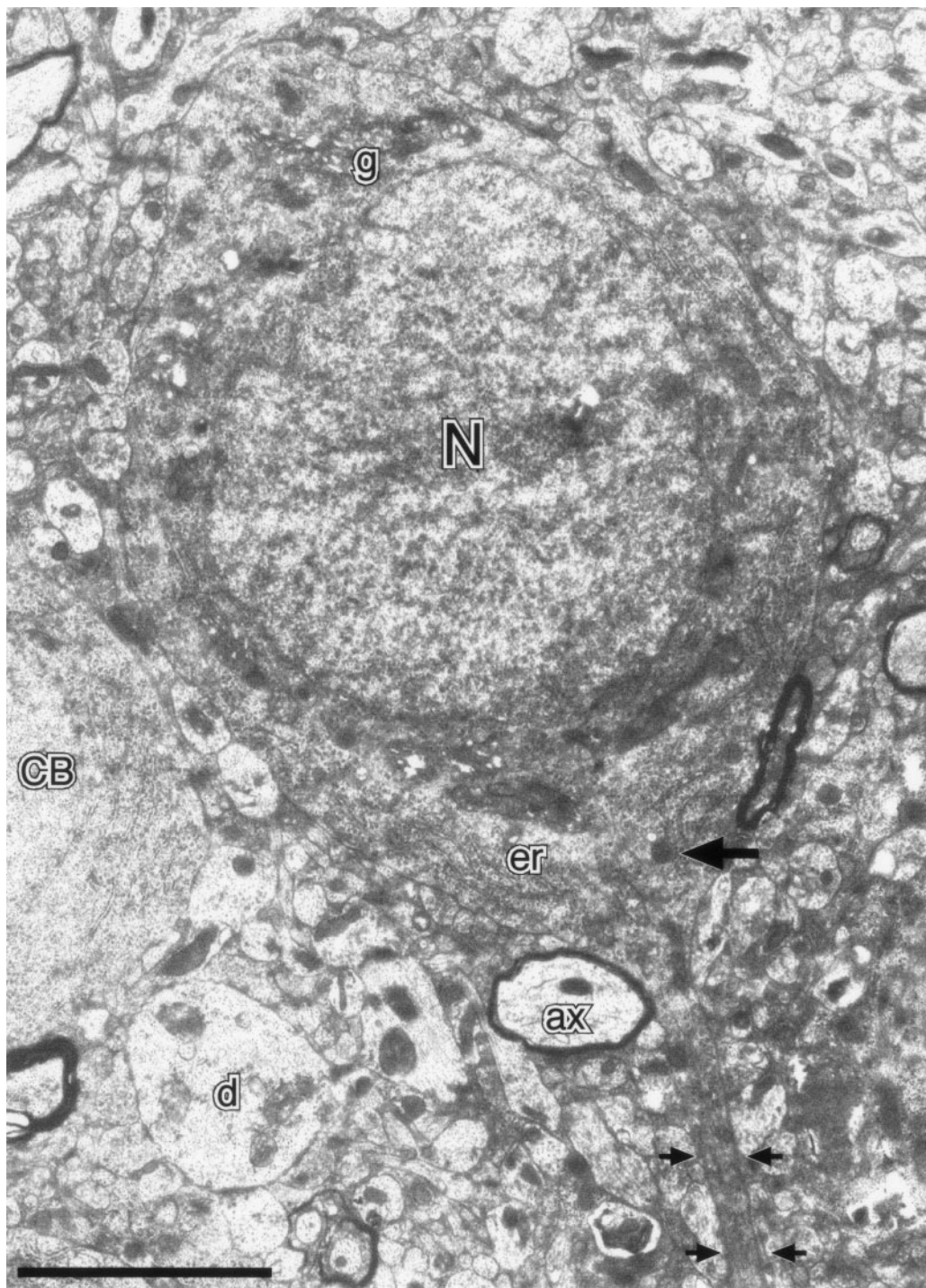

FIG. 2. Electron micrograph of a layer III pyramidal neuron from a control neocortical slice. The nucleus (N) is centrally located and there are numerous organelles in the cytoplasm which appear normal including the Golgi complexes (g) and granular endoplasmic reticulum (er). There are few lysosomes in the cell body (large arrow). Note the axon initial segment (small arrows), which is thin and uniform in caliber, the cell body (CB) of an adjacent neuron, a dendritic process (d), and myelinated axon (ax). Bar, 5 μm.
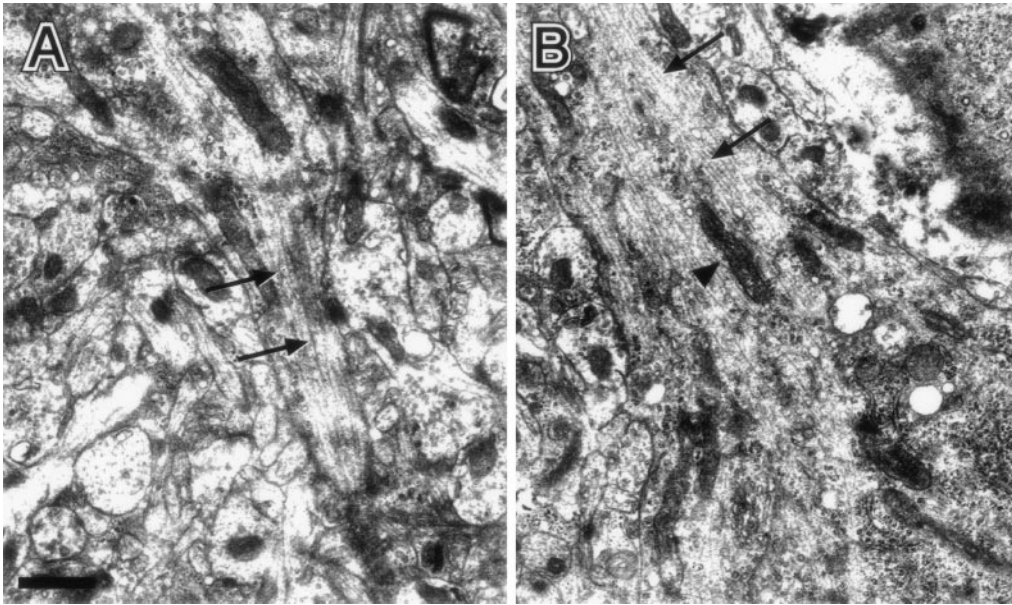
FIG. 3. (A) An electron micrograph of an axon initial segment from a layer III pyramidal cell obtained from a control slice. Note the absence of lysosomes in the axon and the bundles of microtubules (arrows). (B) An enlargement of the apical dendrite from the same cell in (A). The cytosolic organelles including the mitochondria (arrowhead) and microtubules (arrows) are evident. Bar, 1 μm.

adult rats. The perikaryal cytoplasm contained several electron-dense organelles (Fig. 2) that ranged in diameter from 0.26 to 0.39 μm (mean ± SEM; 0.31 ± .04 μm, $n = 24$). Because these organelles did not contain cristae and were surrounded by an electron-lucid halo beneath the single-limiting membrane, they will be referred to as endosomes-lysosomes throughout the remainder of the paper. The axon initial segments (Fig. 3A) were characterized by bundles of microtubules, a constant small diameter, and a dense undercoating of the axolemma. Apical and basal dendrites were covered with well-developed axospinous and axoden-
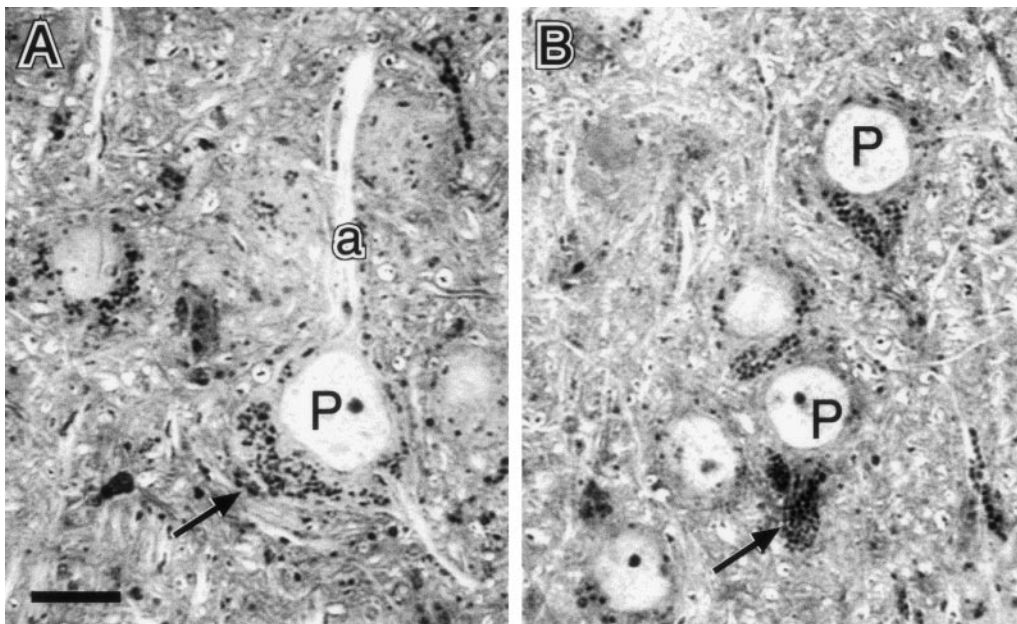
FIG. 4. (A) Light micrograph of a toluidine blue-stained semithin section through layer III of a slice treated with ZPAD for 6 days. A pyramidal neuron (P) has a prominent apical dendrite (a) that contains a few darkly stained granules. Note, that most granules are preferentially located in the basal portion of the soma (arrow). (B) Pyramidal neurons (P) from layer III of a slice treated with ZPAD for 6 days and given 4 days to recover show an accumulation of basophilic granules at the base of each soma with one showing the early stages of a meganeurite (arrow). Bar, 10 μm.
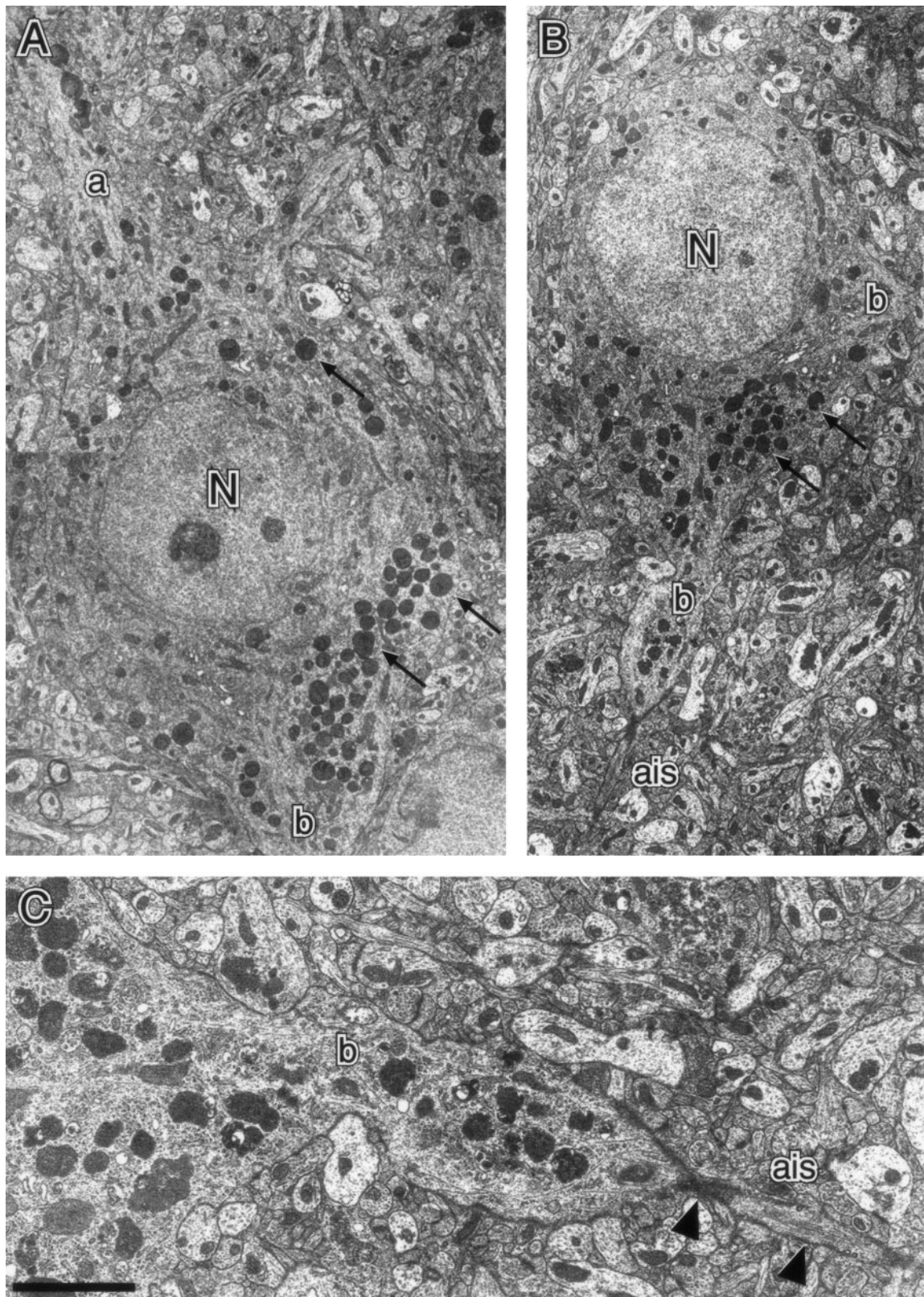
FIG. 5. (A) Electron micrograph of a layer V neuron from a neocortical slice treated with ZPAD for 6 days. The nucleus (N) is located centrally. Lysosomes (arrows) in these neurons are interspersed more evenly throughout the perikaryal cytoplasm than those in layer III pyramidal neurons. The apical dendrite (a) and a basal dendrite (b) are also shown. Meganeurites were not found in neurons in this layer. (B) Layer III pyramidal neurons also show lysosomal proliferation. Again, the nucleus (N) appears normal but unlike the layer V pyramidal neurons, the majority of lysosomes (arrows) have accumulated in the basal portion of the soma. Notice the basal dendrite (b), the axon initial

dritic synapses and contained longitudinally oriented neurofilaments and microtubules (Fig. 3B).

Morphological changes induced by ZPAD. Incubation with 45 μM ZPAD, a dose previously shown to suppress cathepsins B and L without inhibiting the related cysteine protease calpain (3), for 6 days did not disrupt the laminated distribution of cells described above for control slices. Numerous densely stained granules were found in neurons in all layers from toluidine blue-stained semithin sections (Fig. 4A). For most neurons, these dense bodies were homogeneously distributed across the perikaryal cytoplasm and were frequently encountered in dendrites. Layer III cells differed from neurons in deeper layers in that the granules, although present throughout the cell body and proximal dendrites, tended to be concentrated in the basal pole of the somata (Fig. 4A).

Electron microscopic studies showed that the dark granules were larger but ultrastructurally were similar to endosomes-lysosomes of control slices. These electron dense structures ranged in diameter from 0.43 to 0.58 μm (mean ± SEM: 0.52 ± .06, $n = 235$). The increase in the number of these organelles suggested by light microscopy was confirmed in the ultrastructural analysis (Fig. 5). Electron micrographs showed that endosomes-lysosomes of all sizes were not confined to the cell body in the treated slices but were also common in large dendritic branches where they would often form "trains" stretching along the proximo-distal axis of the process. Microtubules were absent or seemingly displaced in many dendritic sites containing groups of endosomes-lysosomes (Fig. 5C). Layer III pyramidal neurons differed from neurons in other laminae in having small but distinct endosome-lysosome filled expansions in the region of the axon hillock (Fig. 5B). Despite the dramatic proliferation of endosomes-lysosomes, mitochondria and other cellular organelles were not noticeably different than those in control slices.

Morphological changes observed after a 4-day recovery period from ZPAD treatment. Slices treated with ZPAD for 6 days and then given four days to "recover" maintained a lamination pattern similar to that seen in control slices. Three obvious changes from the 6-day group were found in layer III. First, pyramidal neurons in this layer showed a reduction in the number of endosomes-lysosomes in their apical dendrites and cell bodies (Fig. 4B; Fig. 6, inset). In contrast, the number of endosomes-lysosomes within the cell bodies and dendrites of layer V pyramidal cells was similar to that found at the end of the 6-day treatment with the

cathepsin inhibitor (not shown). There was also no evidence of clustering in the basal region of the somata in layer V. Second, endosomes-lysosomes in layer III pyramidal neurons were noticeably smaller than endosomes-lysosomes found in slices treated with ZPAD for 6 days. Third, appropriately sectioned layer III neurons contained fusiform expansions of the axon hillock region that were interposed between the cell body and axon initial segment and filled with many endosomes-lysosomes (Fig. 6). These structures contained whorled membranes and vacuoles in addition to individual lysosome-like organelles. In terms of location, size, and contents, the expansions closely resembled protuberances referred to as meganeurites by Purpura and Suzuki (18).

The induced meganeurites varied in size but in some cases had diameters which approached that of the pyramidal cell bodies. The tear drop-shaped meganeurite shown in Fig. 6 was common but numerous other configurations including columnar, conical, and triangular-shaped meganeurites (Fig. 7) were also found. Other than the meganeurites, the layer III neurons appeared surprisingly normal; e.g., spines and synapses were evident on proximal dendrites and axosomatic symmetric synapses were present on the perikarya. Of particular interest, symmetric synapses were sometimes encountered on the proximal portions of the meganeurites as expected if these structures arose from an expansion of the juncture of the cell body and axon. Despite their dense populations of endosomes-lysosomes, pyramidal, and nonpyramidal cells outside of layer III did not appear to form meganeurites.

DNA fragmentation. The TUNEL method, which relies on the *in situ* labeling of DNA breaks (4, 12), was used to detect apoptotic cells. Positive neurons were characterized by stained nuclei (Fig. 8) or stained fragments within nuclei. In control slices, labeled cells were largely confined to the two broad surfaces (i.e., the slice interface exposed to the atmosphere and that attached to the membrane) and were most numerous in layers II/III. Sections through the middle of the slices had little, if any, labeling. The effects of ZPAD on apoptosis were tested after meganeurites were well established; i.e., after a 6-day treatment with the inhibitor plus a 7-day "recovery" period. There were no differences in the number of labeled cells on the surfaces of control ($n = 7$) vs ZPAD-treated slices ($n = 10$), and no evidence for apoptosis existed at greater depths in slices of either group. The incidence of apoptotic cells did not change after more extended recovery periods. Slices treated with ZPAD for 6 days and given an

---

segment (ais), and the presence of lysosomes extending toward this latter process shown in B. (C) An enlargement of the basal dendrite (b) and axon initial segment (ais). The sublemmal dense undercoating (arrowheads), cylindrical shape, and the fasciculation of microtubules in the ais were used for its identification. Bar, 13 μm in A, 9 μm in B, and 2 μm in C.
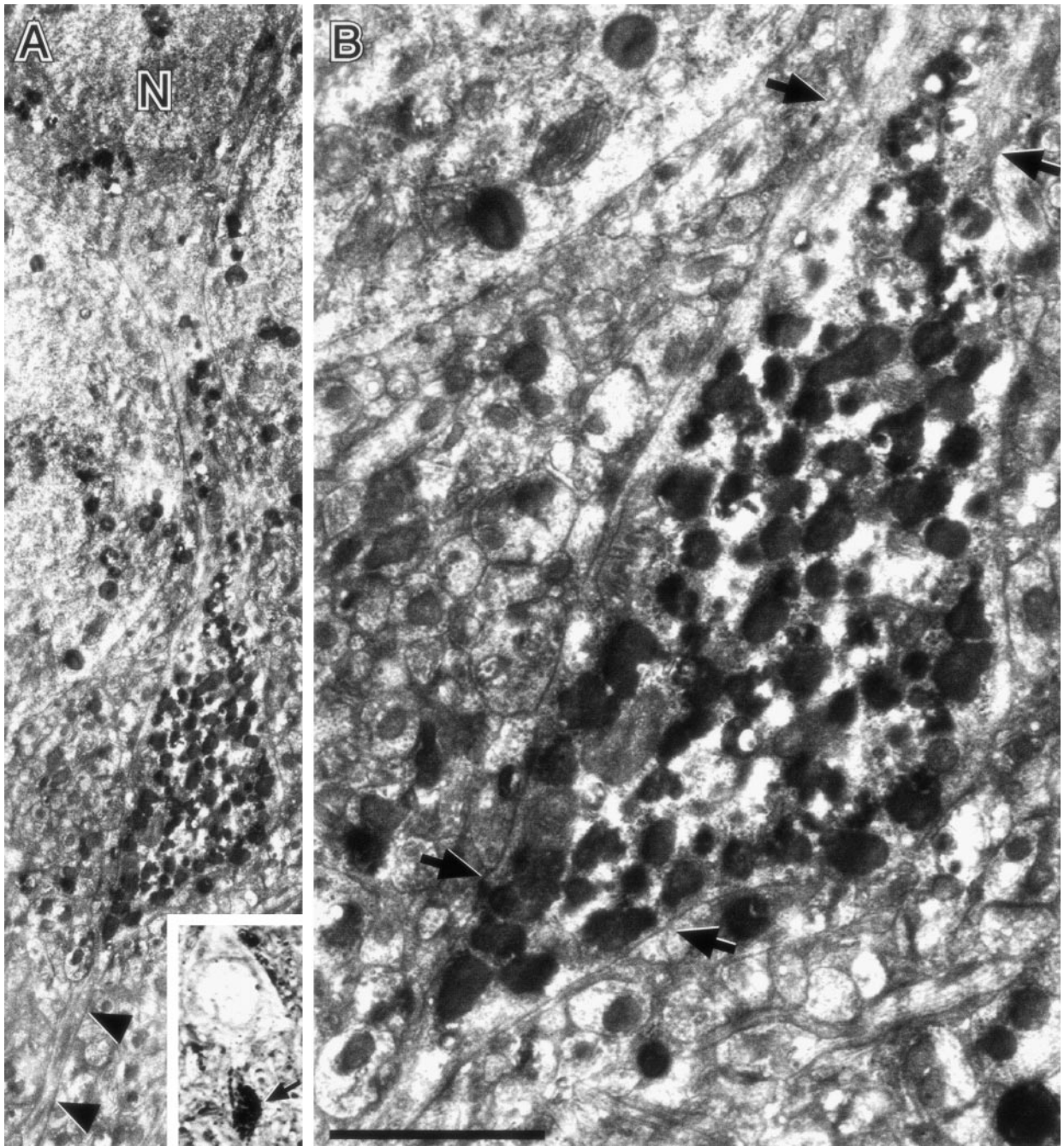
FIG. 6. (A) Montage of electron micrographs of a layer III pyramidal cell from a cultured frontal cortical slice treated with ZPAD for 6 days and given 4 days to recover. The nucleus (N) and cell body appear normal with few lysosomes located in the perikaryal cytoplasm. Note the numerous lysosomes found in the fusiform expansion or meganeurite (arrows in B). The axon initial segment is displaced distally by the meganeurite (arrowheads). Inset, Light micrograph of a layer III pyramidal neuron with a similarly shaped fusiform expansion. (B) An enlargement of the fusiform expansion in A. Endosomes-lysosomes are more heterogeneous in shape than lysosomes found after 6 days of ZPAD treatment because several contain vacuoles. Bar, 6 μm in A, 35 μm in the inset, and 2.5 μm in B.

additional 12 days in standard medium ($n = 10$) did not display an appreciable difference in the number of TUNEL-labeled neurons compared to controls ($n = 7$). Stained nuclei were absent in control and ZPAD-treated slices incubated without terminal transferase ($n = 7$/group for both 7- and 12-day recovery periods).

DISCUSSION

Increased numbers of endosomes-lysosomes were evident in all layers of cortex following 6 days of treatment with the cathepsin B and L inhibitor. This proliferation is probably part of a homeostatic response
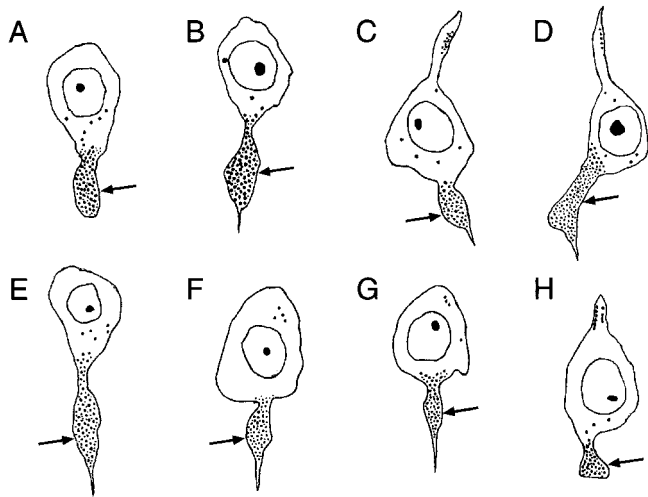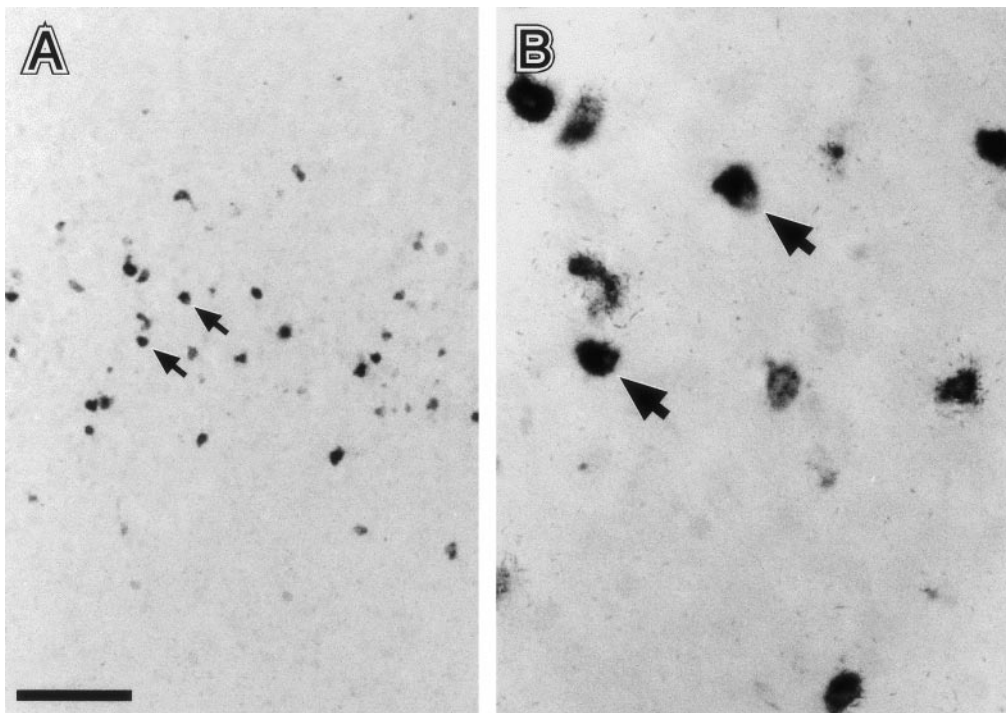
FIG. 7. Camera lucida drawings taken from layer III of slices treated with ZPAD for 6 days and given 4 days to recover. Multiple morphologies of meganeurites were found including those that were columnar (A, B, C, D), conical (E, F, G), and triangular (H) in shape.

washout/recovery period of several days resulted in the development of numerous meganeurites in layer III but not in layer V pyramidal cells. These structures were often very large, approaching the size of the cell body, and displaced the initial segment of the axon distally, away from the perikaryon. Generalized endosome-lysosome proliferation and layer III selective meganeurites characterize the human neocortex in late middle age (5). By reproducing this pattern, the present results support the hypothesis that age-related changes seen in the human brain arise from slowly developing disturbances in lysosomal processing.

Why lysosomal dysfunction induces meganeurites in only some neurons is an essential question for future studies. Prior work showed that cathepsin inhibitors generate these abnormalities in CA1 pyramidal neurons but not elsewhere in hippocampus (3), raising the question of what properties are common to pyramidal cells in CA1 and layer III, but lacking in their adjacent brain areas and layers, respectively. Relative to lysosomes, the most evident shared but atypical characteristic is the relatively prompt removal of the organelles from apical dendrites followed by their accumulation in the basal aspect of the cell body. These events, which are likely due to normally present mechanisms operating on a suddenly expanded population of phagocytotic organelles, do not occur in the larger pyramidal neu-

to subnormal levels of protein breakdown and a degree of amino acid starvation. The latter condition is known to trigger the production of endosomes and phagosomes (19). Proliferation of these organelles was accompanied by a spread of endosomes-lysosomes into dendritic processes. Six days of ZPAD exposure followed by a

FIG. 8. (A) Light micrograph of TUNEL staining in slices treated with ZPAD for 6 days and given an additional 7 days to "recover." TUNEL-positive neurons were confined to layers II/III (arrows); layers I and V to the top and bottom of the photograph, respectively. (B) An enlargement of the TUNEL-positive neurons indicated by arrows in A. TUNEL-positive neurons obtained from the surface of the slice are stained over the entire nucleus (arrows) or over several stained fragments. Bar, 300 µm in A and 100 µm in B.

rons of hippocampal field CA3 and deep neocortex. Possibly, then, the transport processes differ across neuron types with regard to whether they attach and move lysosomes toward the base of the cell. An alternative possibility is that the proliferating organelles differ in some way that affects whether or not they are transported. This could occur if the protolysosomes in layer III arise from a different source, or are exposed to different membrane related enzymes, than is the case for those in neurons in other cortical layers.

While the effects of cathepsin B and L inhibition are in some respects similar in cortical layer III and CA1 pyramidal neurons, differences were also noted. Meganeurites in cortical slices were more irregularly shaped and substantially larger than those in the hippocampus (3). These differences may arise from the relatively tighter packing of neurons in the hippocampal pyramidal cell layer relative to that in neocortex making it possible for adjacent, morphologically similar processes to help shape the cylindrical structure of the meganeurite. Beyond this, meganeurites in CA1 contained fused dense bodies composed of whorled membranes and vacuoles (3), while those in the neocortex did not. This difference is logically related to that just described for size: the smaller meganeurites in field CA1 may lead to tighter packing and, consequently the collapse/fusion of individual organelles. It is noteworthy that lysosomes are reported to remain separated without compaction in the meganeurites found in human frontal cortex (5).

The pyramidal neurons in human frontal cortical layers III and V, in which lysosomal disturbances and neuropathology have been described, are distinguished from their neighbors with regard to their vulnerability in Alzheimer's disease (6, 7, 14). Meganeurites in rat frontal cortical slices were confined to layer III pyramidal neurons, suggesting experimentally induced lysosomal dysfunction at this period of time is not sufficient to generate changes seen in the frontal cortex of the human brain during Alzheimer's. Experiments are now being conducted to determine whether or not longer treatments with the inhibitor or longer recovery periods generate these pathological changes characteristic of AD. However, the possibility still remains that meganeurites may predispose cells to other forms of pathology; e.g., axotomy and rapid cell death are plausible outcomes if cortical neurons attempt to pinch off the blister-like meganeurites. Accordingly, tests were conducted to determine if meganeurite formation by cortical neurons is followed by the appearance of fragmented DNA, one of the distinguishing characteristics of AD (1, 17, 21). No differences in the incidence of apoptotic (i.e., TUNEL-labeled) neurons between control and ZPAD-treated slices were found even when slices were given an extended period of survival after meganeurites had formed. The presence of scattered labeled cells on the surfaces of the slices provided a positive-control for the normal operation of the TUNEL procedure.

It has been suggested that apoptosis may be one possible pathway that leads to neuronal loss in AD. It appears here that modest lysosomal disturbances reproduce pathological features of normal cortical aging but are not of themselves sufficient to generate the broader manifestations of Alzheimer's. Whether more extreme degrees of dysfunction, alone or in combination with other suspected contributors to the disease, elicit appropriately situated apoptosis remains to be determined.

REFERENCES

1. Anderson, A. J., J. H. Su, and C. W. Cotman. 1996. DNA damage and apoptosis in Alzheimer's disease: Colocalization with c-Jun immunoreactivity, relationship to brain area, and effect of postmortem delay. *J. Neurosci.* **16:** 1710–1719.

2. Bednarski, E., and G. Lynch. 1996. Cytosolic proteolysis of tau by cathepsin D in hippocampus following suppression of cathepsins B and L. *J. Neurochem.* **67:** 1846–1855.

3. Bednarski, E., C. E. Ribak, and G. Lynch. 1997. Suppression of cathepsins B and L causes a proliferation of lysosomes and the formation of meganeurites in hippocampus. *J. Neurosci.* **17:** 4006–4021.

4. Ben-Sasson, S. A., Y. Sherman, and Y. Gavriel. 1995. Identification of dying cells—*In situ* staining. In *Methods in Cell Biology* (L. M. Lawrence and B. A. Osborne, Eds.), pp. 29–39. Academic Press, San Diego.

5. Braak, H. 1979. Spindle-shaped appendages of IIIab-pyramids filled with lipofuscin: A striking pathological change of the senescent human isocortex. *Acta. Neuropathol.* **46:** 197–202.

6. Cataldo, A. M., D. J. Hamilton, and R. A. Nixon. 1994. Lysosomal abnormalities in degenerating neurons link neuronal compromise to senile plaque development in Alzheimer disease. *Brain Res.* **640:** 68–80.

7. Cataldo, A. M., D. J. Hamilton, J. L. Barnett, P. A. Paskevich, and R. A. Nixon. 1996. Properties of the endosomal-lysosomal system in the human central nervous system: Disturbances mark most neurons in populations at risk to degenerate in Alzheimer's disease. *J. Neurosci.* **16:** 186–199.

8. Caesar, M., T. Bonhoeffer, and J. Bolz. 1989. Cellular organization and development of slice cultures from rat visual cortex. *Exp. Brain. Res.* **77:** 234–244.

9. Caesar, M., and A. Schuz. 1992. Maturation of neurons in neocortical slice cultures. A light and electron microscopic study on in situ and in vitro material. *J. Hirnforsch.* **33:** 429–443.

10. Cotman, C. W., and J. H. Su. 1996. Mechanisms of neuronal death in Alzheimer's disease. *Brain Pathol.* **6:** 493–506.

11. DeJong, B. M., J. M. Ruijter, and H. J. Romjin. 1988. Cytoarchitecture in cultured rat neocortex explants. *Int. J. Dev. Neuroscience* **6:** 327–339.

12. Gavrieli, Y., Y. Sherman, and S. A. Ben-Sasson. 1992. Identification of programmed cell death *in situ* via specific labeling of nuclear DNA fragmentation. *J. Cell. Biol.* **119:** 493–501.

13. Green, G. D., and E. Shaw. 1981. Peptidyl diazomethyl ketones are specific inactivators of thiol proteinases. *J. Biol. Chem.* **256:** 1923–1928.

14. Hof, P. R. 1997. Morphology and neurochemical characteristics of the vulnerable neurons in brain aging and Alzheimer's disease. *Eur. Neurol.* **37:** 71–81.

15. Kemper, T. L. B., and A. M. Galaburda. 1984. Principles of cytoarchitectonics. In *Cerebral Cortex* (A. Peters and E. G. Jones, Eds.), pp. 35–54. Plenum Press, New York.

16. Landfield, P. W., L. D. Braun, T. A. Pitler, J. D. Lindsey, and G. Lynch. 1981. Hippocampal aging in rats: A morphometric study of multiple variables in semithin sections. *Neurobiol. Aging* **2:** 265–275.

17. Mullaart, E., M. E. T. I. Boerrigter, R. Ravid, D. F. Swaab, and J. Vijg. 1990. Increased levels of DNA breaks in cerebral cortex of Alzheimer's disease patients. *Neurobiol. Aging* **11:** 169–173.

18. Purpura, D. P., and K. Suzuki. 1976. Distortion of neuronal geometry and formation of aberrant synapses in neuronal storage disease. *Brain Res.* **116:** 1–21.

19. Schworer, C. M., and G. E. Mortimore. 1979. Glucagon-induced autophagy and proteolysis in rat liver-mediation by selective deprivation of amino acids. *Proc. Natl. Acad. Sci. USA* **76:** 3169–3173.

20. Stoppini, L., P.-A. Buch, and D. Muller. 1991. A simple method for organotypic cultures of nervous tissues. *J. Neurosci. Methods* **37:** 173–182.

21. Su, J. H., A. J. Anderson, B. J. Cummings, and C. W. Cotman. 1994. Immunohistochemical evidence for apoptosis in Alzheimer's disease. *Neuroreport* **5:** 2529–2533.

22. Vaughan, D. W., and J. M. Vincent. 1979. Ultrastructure of neurons in the auditory cortex of ageing rats: a morphometric study. *J. Neurocytol.* **8:** 215–228.